

Wideband Rectangular Microstrip Patch Antenna Using L-Probe Feeding System

Pavel HAZDRA, Miloš MAZÁNEK, Jiří ČERMÁK

Dept. of Electromagnetic Field, Czech Technical University, Technická 2, 166 27 Praha, Czech Republic

hazdrap@fel.cvut.cz

Abstract. Paper focuses on so-called L-probe feeding technique suitable for wideband ($>30\%$ relative bandwidth) driving of microstrip patch antennas. Physical explanation, simulation and measurement are presented. Further modification for improvement of radiation characteristic is also proposed.

Keywords

Microstrip patch antenna, L-probe, wideband antennas, proximity coupling.

1. Introduction

Microstrip patch antennas are usually designed to have small relative bandwidth (BW), 3-10%. Usually the feeding system is a major bandwidth limitation. L-probe [1] driving technique is able to increase relative BW more than 30% while keeping reasonable radiation properties.

2. Principle of Operation

First let's have a look to the sketch of the patch antenna with the L-probe feed (Fig. 1).

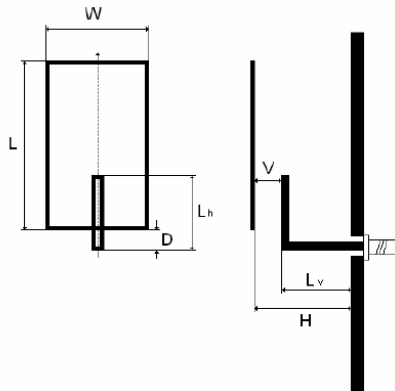


Fig. 1. Rectangular patch antenna with the L-probe feed.

Basically, the structure could be seen as a patch antenna electromagnetically coupled to the L-shaped capacitively loaded monopole. Both the monopole and patch have its

own resonances which, if properly combined, give rise to a broadband behavior. Moreover, L-shaped monopole near field (Fig. 3) coincides with the eigen-field of the TM_{01} patch mode thus effective coupling patch-probe is possible.

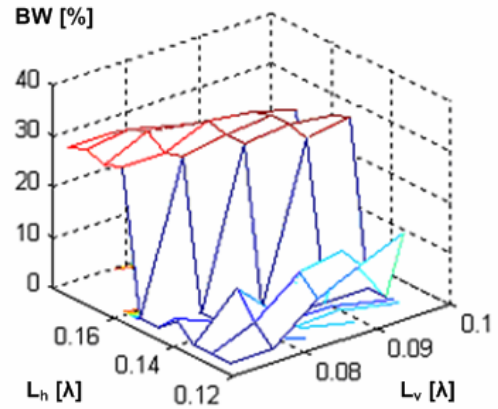


Fig. 2. Parametric analysis on bandwidth.

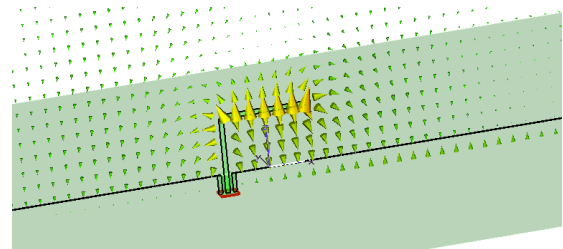


Fig. 3. E field distribution of the L-probe only.

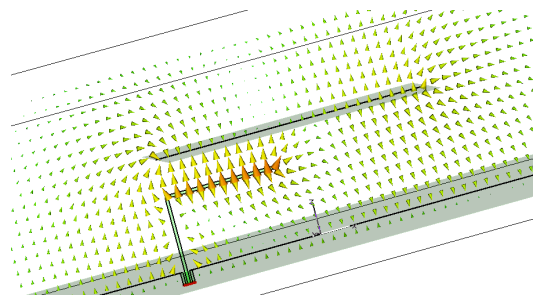


Fig. 4. E field distribution of the L-probe with the patch.

A result of an extensive bandwidth-related parametric study of sample structure with $L = 56$ mm, $W = 37$ mm, $H = 23$ mm and $D = 0$ is shown in Fig. 2. It can be clearly

distinguished how the bandwidth is influenced by a variation of L_v and L_h (described in Fig. 1); the result is shown in Fig. 2. Dielectric used in simulations was air.

From the analysis, we can observe that the biggest relative bandwidth (referred to condition $RL < -10\text{dB}$) is obtained for L_h between $0.14 - 0.19 \lambda_c$ and L_v between 0.08 and $0.11 \lambda_c$. Deeper study gives the best values $L_h = 0.15 \lambda_c$ and $L_v = 0.1 \lambda_s$. So, the complete length of the feeder is equal to the “monopole” length $\lambda_c/4$ (see Fig. 3) at the design frequency f_c (will be discussed later). Consequently, the L-probe system could be viewed as a capacitively loaded monopole electromagnetically coupled to the TM_{01} field under the patch (Fig. 4).

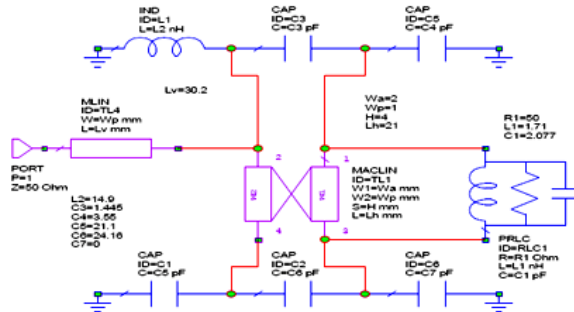


Fig. 5. Equivalent circuit model for the L-probe and the patch.

In order to physically explain the structure behavior, we have proposed the following equivalent circuit (Fig. 6).

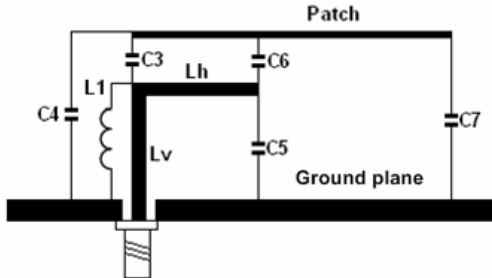


Fig. 6. Parasitic components appearing in the equivalent circuit (some capacitors were merged for clearness).

The patch antenna is modeled as parallel RLC circuit (alternatively it could be represented using a transmission line model [2]) and the L-probe as a stub consisting of 2 ideal lines. Interaction between the patch and the horizontal arm of the feeder is accounted through coupled lines (MACLIN component). Other elements model parasitic components.

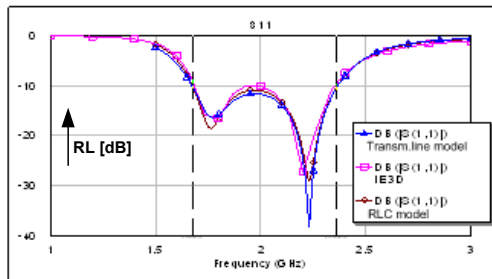


Fig. 7. Return Loss - Equivalent circuit modeling and IE3D full-wave simulation.

Comparison of IE3D [3] full-wave MoM simulation and the equivalent circuit (transmission line and RLC model [2] of the patch) modeling of the RL is shown in Fig. 7.

2.1 Design Guidelines

Based on number of parametric simulations we are able to point out two fundamental steps for the design of the proposed broadband (relative BW~38%) patch antenna with the center frequency f_c . Let us consider dielectric to be air, thus $\lambda_c = c_0/f_c$.

- The design of the rectangular $L \times W$ patch:

The resonant length of the patch L is obtained by the following equation:

$$L = \frac{c_0}{f_c} \frac{3}{8}. \quad (1)$$

The above equation takes into account both the fringing field effect and the fact that the patch resonance has to be shifted below the f_c frequency by roughly 10% in order to obtain broadband behavior.

The width of the patch W isn't a crucial design parameter, however we have determined its optimal value in terms of radiation characteristics to be $W=2/3L$, see also [4].

- The L-probe design:

The optimal BW performance has been obtained for:

$$\begin{aligned} L_h &= 0.15 \lambda_c, \\ L_v &= 0.10 \lambda_c, \\ H &= 0.15 \lambda_c. \end{aligned}$$

(Note that $L_h+L_v=0.25 \lambda_c$.)

To verify the proposed design strategy, several antennas (with different center frequencies f_c) were successfully simulated using relations described above.

3. Results

The example of the L-probe fed patch for $f_c = 2\text{GHz}$:

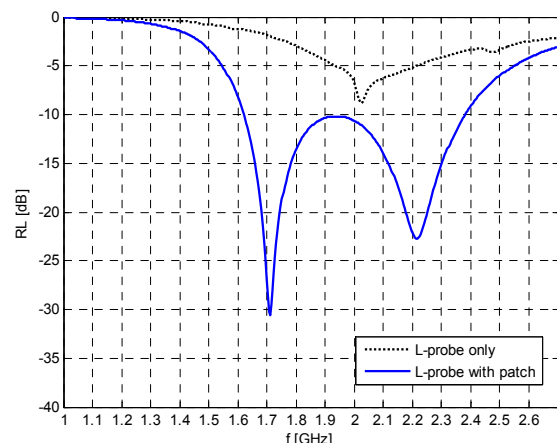


Fig. 8. Calculated Return Loss for alone L-probe and L-probe together with the patch.

Using the equations mentioned above, the optimal dimensions obtained are: $L = 56$ mm, $W = 37$ mm, $L_h = 22.5$ mm, $L_v = 15$ mm and $H = 22.5$ mm.

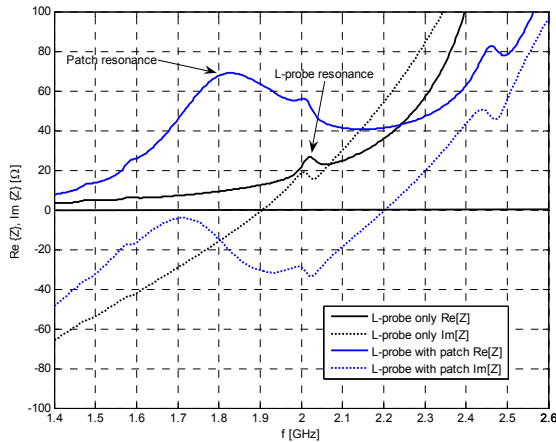


Fig. 9. Input impedance for alone L-probe and for probe + patch.

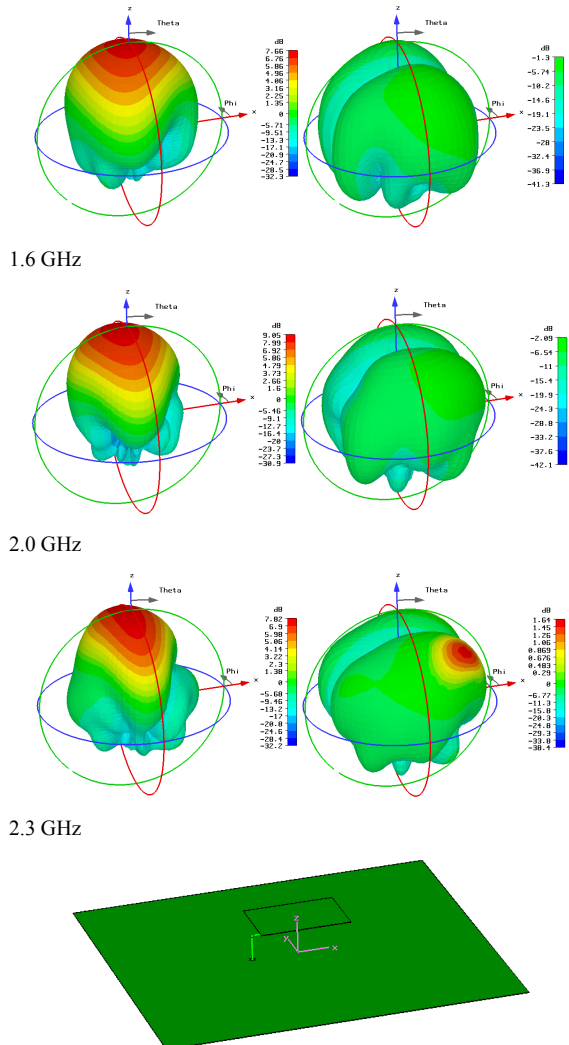


Fig. 10. Original antenna. Co- and cross-polar (Ludwig-3 scheme used) 3D radiation patterns throughout the operating band and structure orientation.

The full-wave simulation results (calculated by the FIT simulator CST-MWS [5] with finite ground plane $1.4 \lambda_c \times 1.4 \lambda_c$) are shown below, see matching in Fig. 8. The relative BW for $\text{RL} < -10$ dB is 38%.

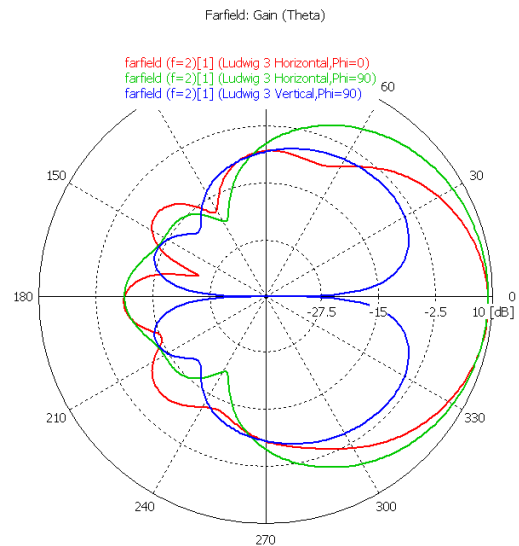


Fig. 11. Original antenna. Polar cuts @ 2 GHz for $\phi = 0^\circ$ and 90° , green+red curves co-polar polarization, blue curve cross-polarization in H-plane.

The input impedance presents an interesting behavior, an imaginary part $\text{Im}\{\mathbf{Z}\}$ of the system L-probe + patch “oscillates” around the 0 value in a quite wide band. This could be explained by electromagnetic coupling probe-patch where their natural resonances are combined (see Fig. 9). This idea was also confirmed by equivalent model simulations.

The calculated 3D far-field patterns are shown in Fig. 10, note a quite higher level of cross-polarization (more comments on that will follow later). Fig. 11 displays main far-field cuts at the center frequency f_c . Cross-polarization shown with blue curve dominates at H-plane (YZ). Cross-polarization in E-plane is less than -40dB and therefore is not shown in the picture.

4. Improved L-Probe Feeder Structure

The simple L-probe fed structure suffers from currents flowing along the vertical part L_v of the feeder. Their effect develops mainly in higher cross-polar level in the H-plane (YZ cut), see Fig. 10. Also the main lobe direction in the H-plane doesn't have its maximum at broadside direction (it is shifted by 5° because of the structure asymmetry). In [6], two out-of-phase fed L-probes are used to improve radiation properties. However, we have found a simpler solution which employs a piece of another properly placed vertical wire as depicted in Fig. 12. The currents induced on this auxiliary wire are out-of phase and thus partially cancel currents [6] on the L_v part and improve radiation properties of the whole structure. An additional wire also helps to improve structure symmetry. Fig. 13

shows that the near electric field distribution remains almost unchanged compared to the original structure (confront with Fig. 4).

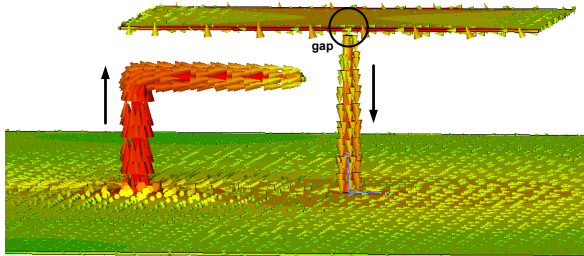


Fig. 12. Surface current density on the improved structure.

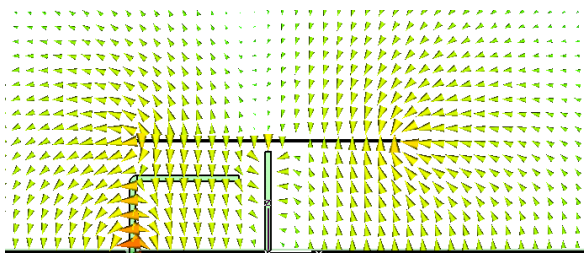


Fig. 13. E-field distribution of the L-probe, wire and patch.

The simulated return loss of both solutions (classical L-probe and improved one with auxiliary wire) is shown in Fig. 14, the input impedance in Fig. 15. It could be noticed that the impedance behavior is almost the same as for the L-probe case. The improved structure has slightly lower relative BW, 34%, compared to 38% of the original antenna with the L-probe only.

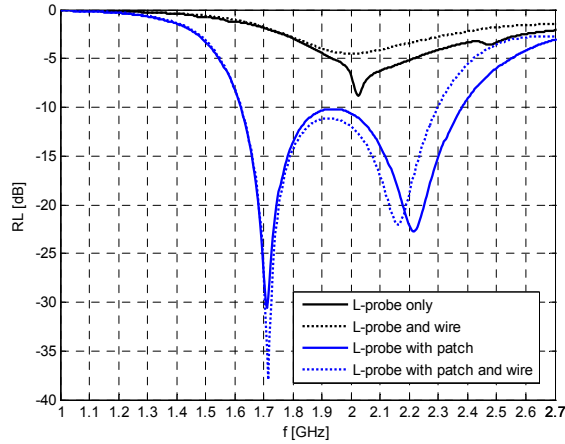


Fig. 14. Return Loss for various combinations of the L-probe, the additional wire and the patch.

Radiation patterns of the improved structure are shown in Fig. 16 and Fig. 17, note significant improvement namely in cross-polar characteristics (see Fig. 10 for axis orientation). It should be emphasized that the maximum radiation is now at broadside (see Fig. 17 and compare it to Fig. 11).

The calculated gains display $G > 8$ dBi in the working band (1.6 – 2.3 GHz) with peak gain 9.2 dBi located at f_c .

The improved structure has the gain enhanced by + 0.3 dB – 0.5 dB, see Fig. 18.

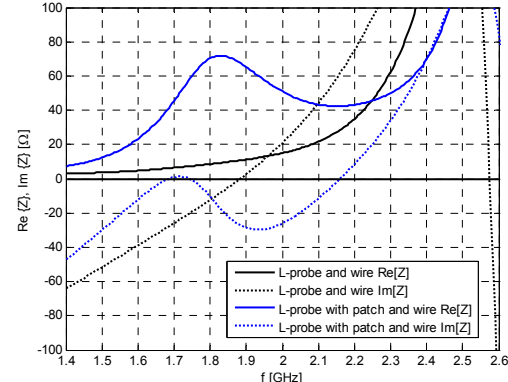


Fig. 15. Input impedance for various combinations of the L-probe, the additional wire and the patch.

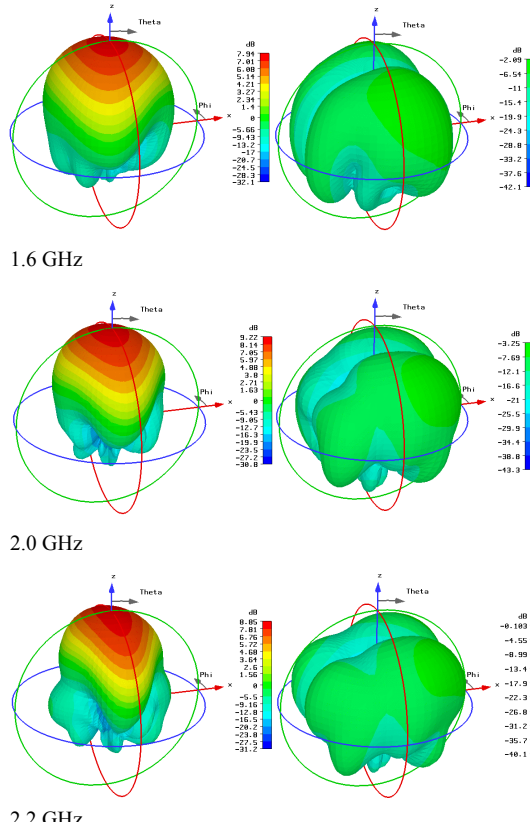


Fig. 16. The improved antenna. Co- and cross-polar (Ludwig-3 scheme used) 3D radiation patterns throughout the operating band.

5. Measured Results

The original antenna (without the additional wire) was manufactured (Fig. 19) and its RL was measured. The antenna was designed for $f_c = 2$ GHz (see dimensions in section 3 of this article) with ground plane 210×210 mm ($1.4 \lambda_c \times 1.4 \lambda_c$), however after manufacturing, quite big differences mostly in L-probe size were found out, Tab.1.

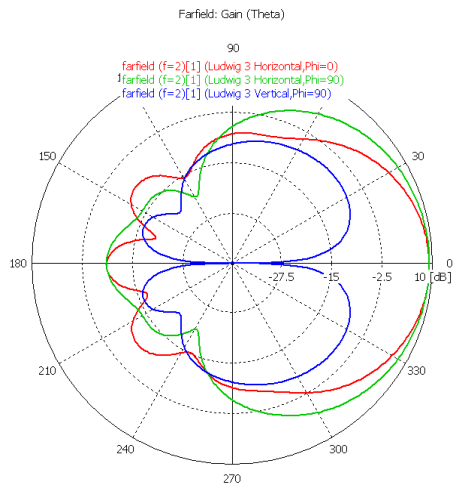


Fig. 17. The improved antenna. Polar cuts @ 2GHz for $\varphi=0^\circ$ and 90° , green+red curves co-polar polarization, blue curve cross-polar in H-plane.

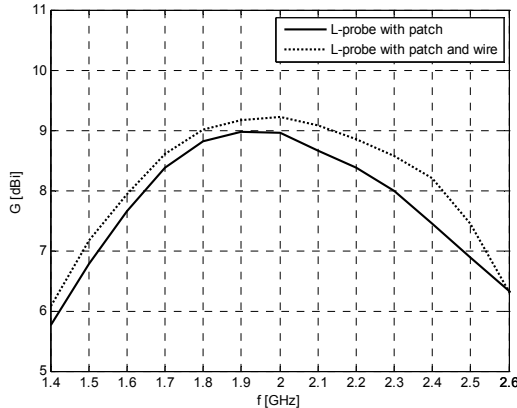


Fig. 18. Calculated gains of the primary (L-probe+patch) and improved (L-probe+patch+wire) structure.

Although the designed and actual manufactured sample dimensions differ, matching is still satisfactory (though at the center frequency RL exceeds -10dB, this is addressed mainly to L_v). After the RL measurement, the whole antenna has been re-simulated with the CST MWS [5], together with distance rollers included, which are used for holding the patch. The comparison between the simulation and the measurement is depicted in Fig. 20.

6. Conclusions

The paper aimed on the design of the wideband patch antenna with the L-probe feeding mechanism. The equivalent circuit has been proposed and the mechanism of operation explained. Such kind of design could provide relative bandwidth more than 30%. Further improvement of radiation properties has been proposed and the sample of the antenna was built and measured as well.

The main advantage of this antenna is reaching (30 to 38%) bandwidth, very low cost, easy fabrication (no need for drilling and soldering the patch) and low sensitivity to manufacturing imperfection.

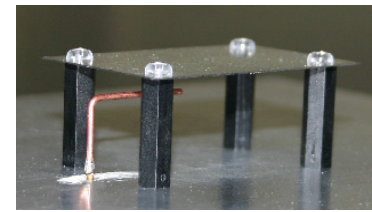


Fig. 19. Detail of the L-probe and the patch.

section	designed [mm]	actual [mm]	difference [mm]	difference [%]
L_h	22.5	23.4	+0.9	+4
L_v	15	17	+2	+13.3
H	22.5	23	+0.5	+2.2
D	0	1.2	+1.2	-
V	7.5	5.7	-1.8	-24

Tab. 1. Designed and actual size of the measured antenna sample.

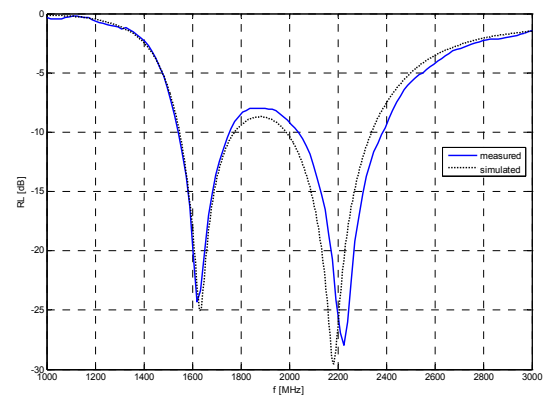


Fig. 20. Measured and simulated results on the L-probe patch antenna.

References

- [1] MAK, C. L., LUK, K. M., LEE, K. F., CHOW, Y. L. Experimental study of a microstrip patch antenna with an L-shaped probe. *IEEE Trans-AP*, 2000, vol. 48, no. 5.
- [2] BAHL, I., BHARTIA, P., GARG, R. *Microstrip Antenna Design Handbook*. Artech House, 2001.
- [3] www.zeland.com
- [4] MAS, Ch. L., WONG, H., LUK, K. W. *High-Gain and Wide-Band Single-Layer Patch Antenna for Wireless Communications*. *IEEE Trans. on Vehicular Technology*, 2005, vol. 54, no. 1.
- [5] www.cst.com
- [6] ZHANG, X-Y., XUE, Q., HU, B-J., XIE, S-L. *A Wideband Antenna with Dual Printed L-Probes for Cross-Polarization Suppression*. IEEE XPLORE.

Acknowledgements

This work has been supported by the Antenna Centre of Excellence (ACE-2) and by the Czech Ministry of Education, Youth and Sports in the framework of the project Research in the Area of Prospective Information and Navigation Technologies MSM 6840770014.